

EVIDENCE OF JET-AMBIENT GAS INTERACTIONS IN THE EMISSION-LINE REGION OF SEYFERT GALAXIES

P. Ferruit

CRAL, Observatoire de Lyon, France

RESUMEN

Flujos colimados (desde viento apenas colimados hasta jets reales) están presentes en una gran variedad de objetos astrofísicos, de los cuales cuatro tipos están representados en este congreso, siendo objetos estelares jóvenes, nebulosas planetarias, radiogalaxias y galaxias Seyfert. En este artículo, primero trataré de dar una breve reseña de las propiedades básicas de los flujos y su ambiente, tal como se observan en estas cuatro diferentes categorías de objetos. Luego regreso a terreno más seguro enfocando hacia mis propios temas de investigación, por ejemplo, el estudio de las interacciones de jets con el medio ambiente en la región de emisión de líneas de galaxias Seyfert, usando la emergente técnica de espectroscopía 3D. Después de listar los diferentes grupos en el mundo que trabajan sobre este tema, presento dos ejemplos de resultados de espectroscopía de campo integral de galaxias Seyfert cercanas (Mrk 573 y NGC 1068). En Mrk 573 datos 3D (x, y, λ) terrestres se usan en combinación con imágenes de alta resolución de *HST* para investigar la naturaleza de arcos y nodos de emisión de líneas observados en este objeto y su relación con el radiojet. Demostramos que en NGC 1068 probablemente hemos encontrado la contraparte óptica del hermoso choque de proa con que termina el radiojet.

ABSTRACT

Collimated outflows (ranging from barely collimated winds to actual jets) are present in a wide range of astrophysical objects, four types of them being represented at this conference, namely young stellar objects, planetary nebulae, radio galaxies and Seyfert galaxies. In this paper, I first try to give a brief overview of the basic properties of the outflows and their environments, as they are observed in these four very different categories of objects. I then go back on safer grounds and focus on my own research topic, i.e., the study of jet-ambient gas interactions in the emission-line regions of Seyfert galaxies, using the emerging techniques of 3D spectroscopy. After listing the various groups working on this subject around the world, I present two examples of results of integral field spectroscopy of nearby Seyfert galaxies (Mrk 573 and NGC 1068). In Mrk 573, the ground-based 3D (x, y, λ) data are used in combination with high spatial resolution *HST* imaging to probe the nature of the emission-line arcs and knots observed in this object and their relationship with the radio jet. In NGC 1068, we show that we have probably found the optical counterpart of the beautiful bowshock which terminates the radio jet.

Key Words: **GALAXIES: ISM — GALAXIES: JETS — GALAXIES: SEYFERT — LINE: FORMATION — SHOCK WAVES**

1. A HITCH-HIKER'S GUIDE TO JETS

Collimated outflows, and in particular jets, are present in a wide range of astrophysical objects. As a consequence, research on these phenomena involves very different communities, which will quite often ignore useful results from other areas. In this context, one extremely interesting aspect (in addition to Caribbean beaches...) of this meeting was that it brought together theorists and observers, working on jets and outflows who came from four different communities, namely the young stellar object, planetary nebula, radio galaxy and Seyfert galaxy communities.

To have a rough idea of how different and/or how similar all these outflows can be, I have tried to summarize their typical characteristics, as well as those of their environments. I have therefore collected the orders of magnitude of a small number of their basic geometrical and physical properties. These quantities are reported in Table 1. In the following I will focus on jets found in nearby active galaxy nuclei (AGN), which, as can be seen in Table 1, extend typically over a kiloparsec scale. They are made of a hot ($\gg 10^6$ K), diffuse medium (the radio plasma) and propagate into the (much cooler and denser) interstellar medium (ISM) of the host galaxy.

TABLE 1
TYPICAL PROPERTIES OF THE JETS AND THEIR ENVIRONMENTS.

	Radiogalaxies	Seyfert galaxies
Size/extent	tens of kpc	\simeq kpc
Jet velocity	relativistic	sub-relativistic
Shock velocities	few thousands of km s^{-1}	hundreds of km s^{-1}
Jet material	hot, diffuse radio plasma (light jet)	hot, diffuse radio plasma (light jet)
Ambient medium	ICM/IGM	ISM
Structure	jet + cocoon	jet + wind ?
Ionizing radiation ?	yes (AGN, stars, shocks)	yes (AGN, stars, shocks)
Distance	very far	far
Line emission	ambient medium	ambient medium
	Herbig-Haro objects	Planetary nebulae
Size/extent	few pc	few tenths of pc to few pc
Jet/wind velocity	few hundreds of km s^{-1}	few thousands of km s^{-1}
Shock velocities	few tens to few hundreds of km s^{-1}	hundreds of km s^{-1}
Jet material	dense, cool gas (heavy jet)	stellar atmosphere
Ambient medium	parent molecular cloud, outflow material	previous outflow material
Structure	jet + loosely collimated wind (molecular)	interacting winds + FLIERs (ejecta ?)
Ionizing radiation ?	yes (accretion region, stars)	yes (central star)
Distance	so close ...	so close ...
Line emission	jet & ambient medium	wind & ambient medium

2. JET-AMBIENT MEDIUM INTERACTIONS IN SEYFERT GALAXIES.

As mentioned above, the material of the jets of Seyfert galaxies is extremely hot and diffuse. The dominant sources of radiative losses in this plasma are not collisionally excited emission-lines or hydrogen recombination, but the free-free and synchrotron processes, the continuum radiation usually observed at radio wavelengths. As a consequence, the jet itself is usually not seen at all at optical or near-infrared wavelengths (contrary to what happens in young stellar objects and planetary nebulae).

Despite this, many Seyfert galaxies exhibit narrow-line regions (NLRs), which are closely associated both morphologically (Haniff, Wilson, & Ward 1988; Capetti et al. 1996; Falcke et al. 1996; Falcke, Wilson, & Simpson 1998) and kinematically (e.g., Whittle et al. 1988; Pécontal et al. 1997) to the ra-

dio emission. One way to explain this association is simply that this line emission is due to the interaction between the jet material and the ISM of the host galaxies. In this scenario, the line emitting gas can either be, shocked gas (in which case the association must be both morphological and kinematical) or unperturbed ISM gas, located ahead of the shocks and ionized by photons generated in the shocks (the so-called precursor; in which case the association is only morphological).

The picture grows more complex when we introduce the effects of the (collimated) ionizing radiation from the central engine. We end up with four possible scenarios, with very different energy budgets:

1. The line emitting gas is predominantly shocked, collisionally ionized gas (*no* photoionization). This scenario, in which the gas is relatively hot (several 10^4 K) is inconsistent with the typically

observed [O III] temperatures ($< 2 \times 10^4$ K, see, e.g., Wilson, Binette, & Storchi-Bergmann 1997) and is therefore ruled out.

2. The shock contribution to the energy budget dominates and the line-emitting gas (which can be precursor gas as well as cooled, dense post-shock gas) is ionized by photons generated *in-situ* in the hot shocked gas. This scenario is actively supported by M. Dopita (see Dopita 2002, these proceedings), who has developed, in collaboration with R. Sutherland, models of such “auto-ionizing” shocks (Dopita & Sutherland 1995, 1996), which are now widely used.

3. The shocks are there but the central engine contribution dominates. In this scenario, the line-emitting gas is mainly post-shock gas photoionized by the nucleus. Although the shocks are not dominant energetically, they dictate the observed morphology of NLR. Indeed the compressed, post-shock gas (which is located in the immediate vicinity of the shocks themselves) will have a higher surface brightness in line emission than the surrounding, more diffuse ISM and will therefore be preferentially detected and observed. Models corresponding to this situation have been developed very early by Viegas-Aldrovandi & Contini (1989, and references therein).

4. The shocks are not there, only the nuclear ionizing radiation. This situation is probably occurring in the extended narrow line region (ENLR) of Seyfert galaxies located further away from the nucleus than the radio jet (and therefore from the associated shocks). The models relevant to this situation are “pure” photoionization models, like the two-component models developed by L. Binette (Binette, Wilson, & Storchi-Bergmann 1996). A large part of the observations of the NLR and ENLR of Seyfert galaxies conducted in the last decade has in fact aimed at discovering for a handful of paradigmatic objects which of these scenarios is the correct one. Comparison between various shock and photoionization models (e.g., Morse, Raymond, & Wilson; Allen, Dopita, & Tsvetanov 1998) had first pointed out diagnostics involving faint UV lines as the best discriminative diagnostics. However, these faint lines are very difficult to observe, are very sensitive to reddening and have not proved as useful as expected (e.g., Ferruit et al. 1999b). Several groups have therefore decided to explore an alternative way. They have engaged in programs of 3D (x, y, λ) spectroscopy of the emission-line regions of nearby Seyfert galaxies in the visible or the near-infrared. These observations provide simultaneous information on the line ratios (classical diagnostics)

and the ionized gas morphology and kinematics (additional discriminative information).

3. WHO’S WHO

I have attempted the hazardous exercise (especially in such a quickly growing community...) of enumerating the various groups in the optical and near-infrared 3D community working in the field of nearby AGN.¹ So far, I can identify six major groups. Bearing witness to the fact that 3D spectroscopy is still not completely democratized, they are all closely associated with the groups responsible of the development of the instruments. These groups are (in random order):

1. The Spanish group lead by S. Arribas and E. Mediavilla (IAC, Spain) who use the fiber-based integral field spectrograph INTEGRAL (Arribas et al. 1998), mounted at the William-Herschel telescope (WHT).

2. A group of Fabry-Pérot instrument adepts which includes S. Veilleux and G. Cecil (see their contributions in the proceedings of this conference).

3. The Japanese group (the “Kyoto” group) lead by H. Ohtani, and organized around a succession of two 3D instruments: 3D-I (Ohtani et al. 1994, 1998) which includes a Fabry-Pérot, as well as a TIGER-type (Bacon et al. 1995) integral field spectrograph; 3D-II (Sugai et al. 1998) with similar, but upgraded modes.

4. The group, including R. Maiolino and N. Thatte, working with the near-infrared instrument called “3D” (Weitzel et al. 1996) which is used in combination with an adaptive optic system.

5. A Russian group lead by V. Afanasiev and organized around a fiber+lenslet-based instrument called MPFS (see Afanasiev & Sil’chenko 2000, and references therein), mounted on the SAO 6-m telescope.

6. The TIGER group (lead by R. Bacon and including E. Pécontal and myself for the nearby AGNs) based at the Lyon observatory and organized around a succession of TIGER-like (Bacon et al. 1995) instruments: TIGER, OASIS and SAURON.

Happily, this still relatively small community is quickly growing as a number of 3D instruments have been commissioned during the last two years and as most 8-m class telescopes include 3D spectrographs as a standard part of their future instrumentation.

¹This restriction to the optical and near-infrared domains excludes radio and X-ray astronomers who have operated 3D instruments since long before optical and near-infrared ones.

4. EXAMPLES OF 3D OBSERVATIONS OF NEARBY AGN

I have chosen to present two different examples of 3D observations of nearby AGN to illustrate what we can learn on the properties of the emission-line regions of Seyfert galaxies and their relationship to the radio jets, from optical and/or near-infrared 3D spectroscopy. First, in Mrk 573, I will show how the ground-based 3D (x, y, λ) data are used in combination with high spatial resolution *HST* imaging to probe the nature of the emission-line arcs and knots observed in this object and their relationship with the radio jet. Second, in NGC 1068, I will show that we have probably found the optical counterpart of the bowshock which terminates the radio jet.

4.1. *The Knots and Arcs of Mrk 573*

4.1.1. *The Data*

The 3D observations of Mrk 573 have been obtained using the TIGER integral field spectrograph (Bacon et al. 1995), mounted on the Canada France Hawaii telescope. They included the $H\beta$, [O III], [N II], $H\alpha$ and [S II] emission lines. Details on the observations and their data reduction can be found in Ferruit et al. (1999a). These originally seeing-limited observations ($0''.9$ – $1''.0$ resolution), have been deconvolved, yielding a final resolution of $0''.35$. In our analysis, we also made use of archival images of the *Hubble Space Telescope*, which had been published in Capetti et al. (1996) and Falcke et al. (1998).

4.1.2. *Evidence for the Presence of Jet/Ambient Medium Interactions*

The presence of jet/ambient medium interactions in Mrk 573 were already suggested by the detection of wings in the [O III] emission-line in the vicinity of the radio lobes (Whittle et al. 1988; Tsvetanov & Walsh 1992). Thanks to our high spatial resolution and our extensive spatial coverage, we have been able to confirm unambiguously the direct association between the radio material and the presence of kinematically disturbed ionized gas. In Figure 1, we show the [O III] $\lambda 5007$ velocity field inferred from our deconvolved data cube with contours of the 3.6-cm radio map (Falcke et al. 1998) superimposed. Each knot in the radio map is spatially associated with a knot in the *HST* emission-line images and with a perturbation in the velocity field of the ionized gas (and vice versa). Figure 2 shows that the [O III] profiles at the location of the radio knots are not only shifted in velocity, but also much broader, with extended wings. All this indicates that we are witnessing the interaction of the radio jet with the ISM of

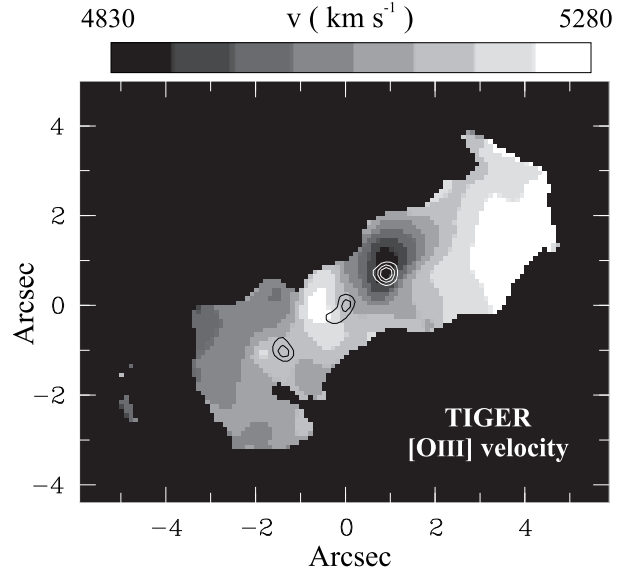


Fig. 1. [O III] $\lambda 5007$ centroid velocity map (gray-scale image) derived from single component Gaussian fitting of the deconvolved TIGER [O III] data cube, with contours of the 3.5 cm radio map at 0.5 , 1 and $1.5 \text{ mJy (beam)}^{-1}$ superimposed.

the host galaxy, and that these interactions modify significantly the kinematics of the ionized gas. However, our data did not allow us to probe the origin of the ionization of the gas in the knots or to discriminate between central source and shock-induced photoionization.

4.1.3. *The Nature of the Arcs*

The arcs of emission observed in Mrk 573 have long been thought to be bow shocks and to trace the location of the interaction between the radio jet and the ISM. Our data have shown that the strongest interactions occur *inside* the arcs (see previous section) and that if shocks are present in the arcs (i.e., if they are actually bow shocks), they must be relatively slow, not to show up in the kinematics of the ionized gas. As the arcs are more extended and located further from the nucleus than the knots, we have been able to use emission-line ratios to probe the origin of the ionization of the gas in these structures.

We have first tested if central source photoionization was viable. From the [N II]/ $H\alpha$ and [S II]/ $H\alpha$ line ratios and using simple photoionization models, we have computed maps of the ionization parameter of the gas. Using the density (derived from the [S II] line ratio), we have then been able to obtain the dependance of the ionizing photon flux with the

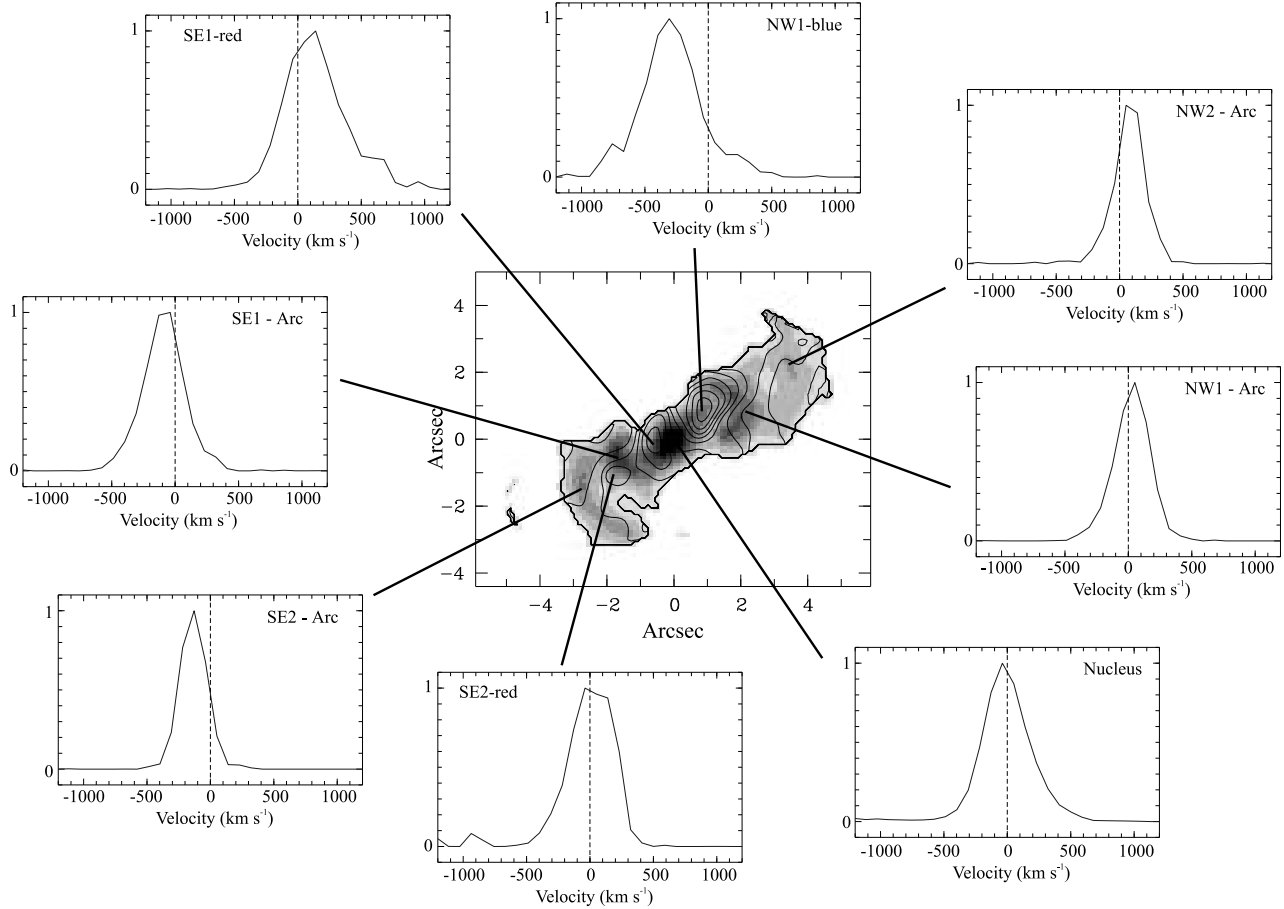


Fig. 2. Central image: [O III] $\lambda 5007$ emission-line map reconstructed from single component Gaussian fitting of the TIGER deconvolved data cube, with the [O III] isovelocity contours superimposed. Profiles: [O III] $\lambda 5007$ velocity profiles from eight selected locations.

radius from the nucleus. If we assume that these ionizing photons come from the central engine and correct for geometrical dilution, we find that the production rate of ionizing photon of the central source necessary to explain the ionization state of the gas, increases by more than a factor ten between radii of $1''$ and $4''$. This indicates that, unless the central source of ionizing photons has varied in the last 4000 years, central source photoionization is negligible in the arcs.

We have then checked if the arcs could be photoionizing shocks. From the comparison between the observed properties of the arcs (luminosity and line ratios) and the predictions of the models of Dopita & Sutherland (1995, 1996), we infer shock velocities of $400\text{--}500\text{ km s}^{-1}$, pre-shock densities $> 10\text{ cm}^{-3}$ and magnetic parameters of $2\text{--}4\ \mu\text{G cm}^{3/2}$. Photoionizing shocks with these velocities and pre-shock densities have specific predicted kinematical and geometrical properties, which remain mostly unused despite

the fact that they provide powerful additional diagnostics (as long as the basic shock parameters are already known). If we apply these diagnostics to the arcs of Mrk 573, we find that they cannot be photoionizing shocks. Indeed, the observed kinematics of the “low” ionization lines (like [N II], [S II] or $\text{H}\alpha$) do not show the expected disturbed kinematics.² In addition, for this range of velocities and pre-shock densities, the precursor should be at least marginally resolved in *HST* observations and the arcs should show different morphologies in [O II] and [O III]. This is not the case in the FOC images (Capetti et al. 1996). Photoionizing shocks are therefore ruled out.

The source of the ionizing photons of the arcs must therefore be searched somewhere else than in the nucleus or inside the arcs themselves. Young, hot

²In the photoionizing shock models, medium ionization lines like [O III], which are predominantly produced in the quiescent precursor, are not expected to exhibit kinematical signatures of the shocks.

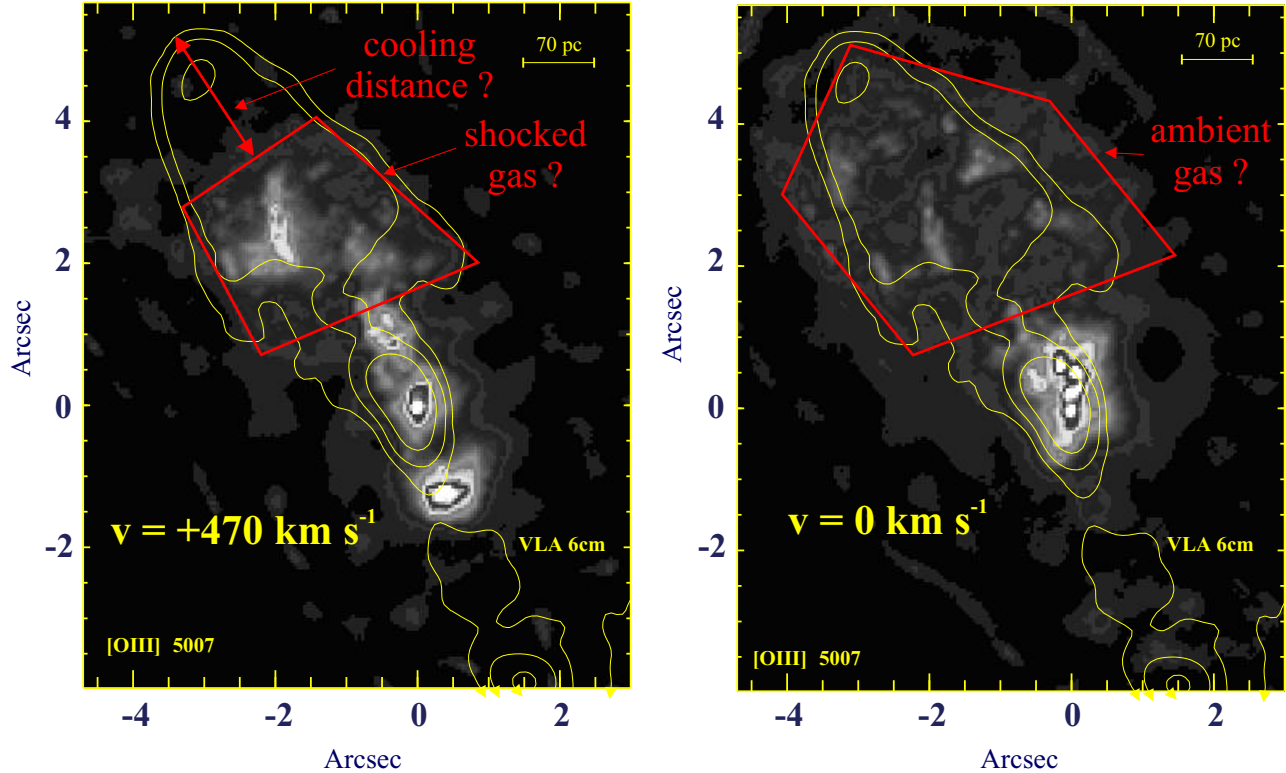


Fig. 3. [O III] images of the bow shock region of NGC 1068 in two different velocity channels ($+470 \text{ km s}^{-1}$, left panel; systemic, right panel) with contours of the 6-cm radio map superimposed.

stars being also ruled out, the best remaining candidate is the hot gas produced in the strong shocks occurring *inside* the arcs (at the location of the knots, see previous section). High spatial resolution spectroscopy and/or observations of high ionization lines are now needed to test this scenario.

4.2. The Bow Shock of NGC 1068

The presence of a bow shock at the termination of the jet of NGC 1068 is known from early 6-cm radio observations (Wilson & Ulvestad 1987). At radio wavelengths, this bow shock is extremely well-defined and this contrasts with the mix of clumpy and filamentary structures observed in optical emission-lines (Machetto et al. 1994; Capetti, Axon & Macchetto 1997). In Figure 3, we show [O III] emission-line maps in two different velocity channels, derived from *deconvolved* TIGER observations of NGC 1068 (for details on the deconvolution of this data cube, see Pécontal et al. 1997). The gas observed in the bow-shock region north of the nucleus, in the $+470 \text{ km s}^{-1}$ channel map (left panel) is confined *inside* and *at the bottom* of the radio contours (little or no [O III] emission is seen close to the apex of the bow shock in this map). On the contrary,

the [O III] emission at systemic velocity (right panel) extends slightly beyond the radio contours, which it fills completely.

These observations suggest a scenario in which the $+470 \text{ km s}^{-1}$ channel gas (confined inside the bow shock structure) is shocked gas flowing along the bow shock. The fact that no [O III] emission is seen close to the apex in this map is consistent with the predictions of the bow-shock model of Ferruit et al. (1997). A plot of the predicted luminosity profile of a 700 km s^{-1} bow shock in emission lines of various ionization levels is shown in Figure 4 (top and middle panels). It can be clearly seen that the emission of medium to low ionization lines (including [O III] $\lambda 5007$) starts $\simeq 40 \text{ pc}$ after the apex (located at $Z = 0 \text{ pc}$). Between 0 and 40 pc, only high ionization lines like [Fe XIV] are present (and marginally [Fe VII]). This is due to the fact that the first particles of cool gas appear only at $\simeq 40 \text{ pc}$. This can be seen in the bottom panel which displays the entrance position of gas particles as a function of their cooling position. All the particles have cooling positions *beyond* 40 pc and therefore only hot gas with temperature incompatible (too high) with the emission of the [O III] line is found before 40 pc.

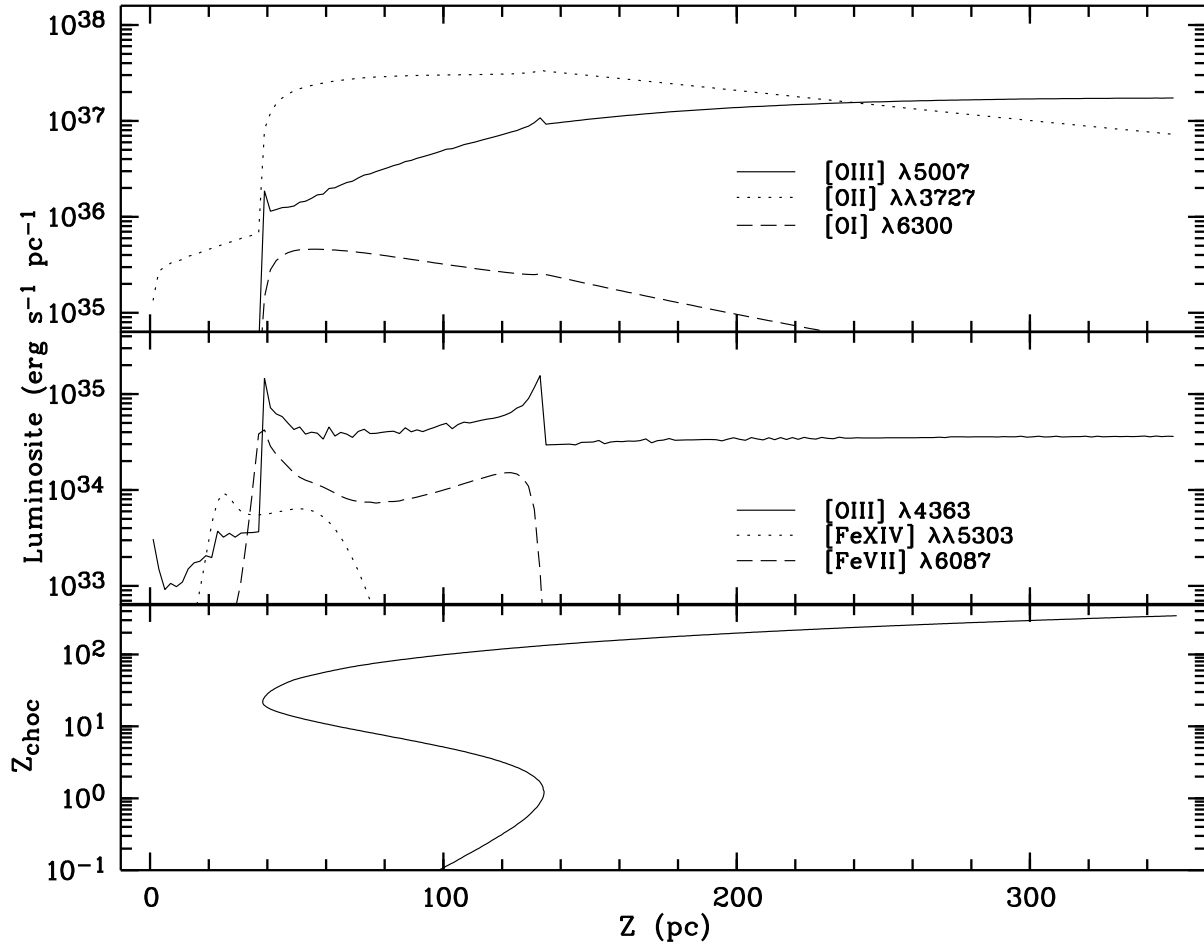


Fig. 4. Luminosity profile of a 700 km s^{-1} bow shock in lines of various ionization levels (upper and middle panels). The bottom panel gives the entrance position Z_{shock} of a particle in the bow shock as a function of its cooling position Z_{cooling} (position where the temperature of the particle cools down abruptly from temperatures above few 10^5 K to temperatures around 10^4 K).

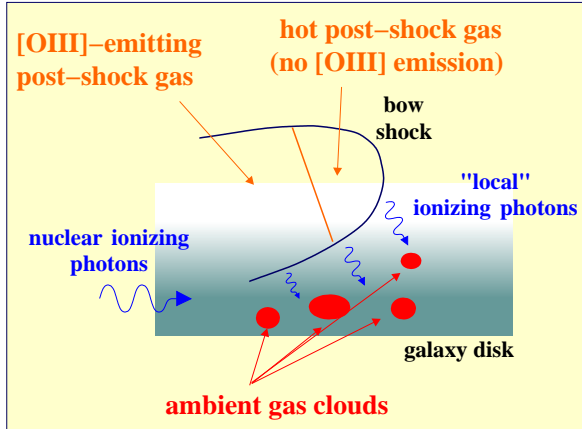
In this scenario, the fact that [O III] emission at systemic velocity is only found in the vicinity of the bow shock structure can be explained if the [O III] emitting gas is ionized by photons produced in the bow shock. A simple sketch of the proposed scenario is shown in Figure 5 (left panel). A slightly different scenario has been proposed by Maiolino et al. (2000). These authors suggest that the low ionization lines are emitted by regions of the bow shock which propagate in the (dense) gas of the galaxy disk, while the high ionization lines are emitted by regions which propagate above the galaxy plane (diffuse gas which will have difficulties to cool after going through the bow shock). Our scenario (contrary to the scenario of Maiolino et al.) predicts that the high ionization lines will be confined to regions close to the apex of the bow shock. Observations of coronal lines like

[Fe XIV] could therefore help to discriminate between these two scenarios.

5. CONCLUSION

Although these two examples show that 3D spectroscopy is an extremely promising tool for the study of the emission-line regions of Seyfert galaxies, current studies have been limited to few individual objects. This is mainly a problem of manpower and a direct consequence of the fact that 3D spectroscopy is still not "democratized". As 3D instrumentation (more instruments, more users \rightarrow more manpower), this situation should change rapidly and observations of actual samples of Seyfert galaxies should become a reality (e.g. as it is already the case in stellar dynamics with the work of the SAURON project).

a



b

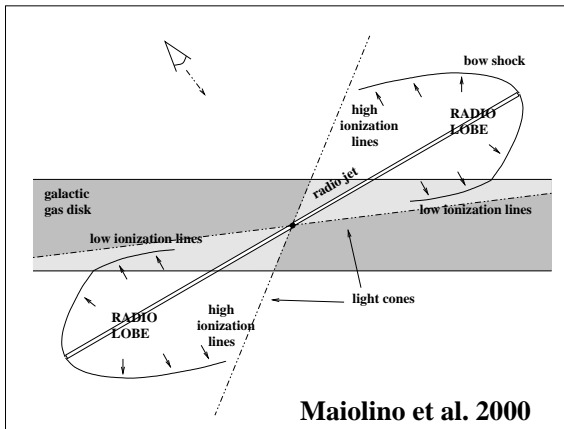


Fig. 5. (a) Sketch of the scenario proposed in this paper to explain the morphology of [O III] emission in different velocity channels shown in Fig. 3. (b) Sketch of a slightly different scenario proposed by Maiolino et al. (2000).

This work received partial support from the conference organizers. Based on observations with the NASA/ESA *Hubble Space Telescope* obtained at the Space Telescope Science Institute, which is operated by the Association of Universities for Research in Astronomy, Inc., under NASA contract NAS 5-26555, and on observations collected at the Canada-France-Hawaii Telescope, which is operated by CNRS of France, NRC of Canada and the University of Hawaii.

REFERENCES

- Afanasiev, V. L.; & Sil'chenko, O. K. 2000, *AJ*, 119, 126
 Allen, M. G., Dopita, M. A. & Tsvetanov, Z. I. 1998, *ApJ*, 493, 571
 Arribas, S., et al., 1998, *Proc. SPIE*, 3355, 821
 Bacon, R., et al. 1995, *A&AS*, 113, 347
 Binette, L., Wilson, A. S. & Storchi-Bergmann, T. 1996, *A&A*, 312, 365
 Capetti, A., Axon, D. J. & Macchetto, F. D. 1997, *ApJ*, 487, 560
 Capetti, A., Axon, D. J., Macchetto, F., Sparks, W. B. & Boksenberg, A. 1996, *ApJ*, 469, 680
 Dopita, M. A. 2002, *RevMexAA(SC)*, 13, 177 (this volume)
 Dopita, M. A., & Sutherland, R. S. 1995, *ApJ*, 455, 468
 ———. 1996, *ApJS*, 102, 161
 Falcke, H., Wilson, A. S., & Simpson, C. 1998, *ApJ*, 502, 199
 Falcke, H., Wilson, A. S., Simpson, C., & Bower, G. A. 1996, *ApJ*, 470, L31
 Ferruit, P., Binette, L., Sutherland, R., & Pécontal, E. 1997, *A&A*, 322, 73
 Ferruit, P., Wilson, A. S., Falcke, H., Simpson, C., Pécontal, E., & Durret, F. 1999a, *MNRAS*, 309, 1
 Ferruit, P., Wilson, A. S., Whittle, M., Simpson, C., Mulchaey, J. S., & Ferland, G. J. 1999b, *ApJ*, 523, 147
 Haniff, C. A., Wilson, A. S., & Ward, M. J. 1988, *ApJ*, 334, 104
 Maiolino, R., Thatte, N., Alonso-Herrero, A., Lutz, D., & Marconi, A. 2000, in *ASP Conf. Ser. 195, Imaging the Universe in Three Dimensions*, eds. W. van Breugel & J. Bland-Hawthorn (San Francisco: ASP), 307
 Morse, J. A., Raymond, J. C., & Wilson, A. S. 1996, *PASP*, 108, 426
 Ohtani, H., et al. 1994, in *Instrumentation in Astronomy VIII*, *SPIE Symp.*, vol. 2198, 229
 Ohtani, H., et al. 1998, in *Optical Instrumentation in Astronomy*, *SPIE Symp.*, vol. 3355, 750
 Pécontal, E., Ferruit, P., Binette, L., & Wilson, A. S. 1997, *Ap&SS*, 248, 167
 Viegas-Aldrovandi, S. M., & Contini, M. 1989, *ApJ*, 339, 689
 Sugai, H., et al. 1998, in *Proc. SPIE Vol. 3355, Optical Instrumentation in Astronomy*, ed. S. D'Odorico (Bellingham, WA: SPIE), 665
 Tsvetanov, Z., & Walsh, J. R. 1992, *ApJ*, 386, 485
 Weitzel, L., et al. 1996, *A&AS*, 119, 531
 Whittle, M., Pedlar, A., Meurs, E. J. A., Unger, S. W., Axon, D. J., & Ward, M. J. 1988, *ApJ*, 326, 125
 Wilson, A. S., Binette, L., & Storchi-Bergmann, T. 1997, *ApJ*, 482, L131
 Wilson, A. S., & Ulvestad, J. 1987, *ApJ*, 319, 105

P. Ferruit: CRAL, Observatoire de Lyon, 9 avenue Charles André, 69561 Saint-Genis-laval cedex, France (pierre@obs.univ-lyon1.fr).